



Study of modification of the magnetic and magnetocaloric properties with Gd doping in Sm-Sr based manganite compounds: Influence of short range charge-orbital ordering

Dipak Mazumdar^{a,*}, Kalipada Das^b, I. Das^c

^a CMP Division, Saha Institute of Nuclear Physics, HBNI, 1/AF-Bidhannagar, Kolkata 700 064, India

^b Department of Physics, Seth Anandram Jaipuria College, 10, Raja Naba Krishna Street, Kolkata 700005, India

^c CMP Division, Saha Institute of Nuclear Physics, HBNI, 1/AF-Bidhannagar, Kolkata 700 064, India

ARTICLE INFO

Keywords:

Manganites
Magnetocaloric effect
Meta-magnetic transition
Relative cooling power
Refrigerant capacity
Charge/orbital ordering

ABSTRACT

Detail investigation on the influence of Gd-doping both in the magnetic and magnetocaloric properties of $(\text{Sm}_{1-y}\text{Gd}_y)_{0.55}\text{Sr}_{0.45}\text{MnO}_3$ ($y = 0.5$ and 0.7) compounds has been carried out. With the Gd-content, the studied compounds exhibit quite distinct physical properties in the presence of an external magnetic field. In addition to the field-induced meta-magnetic transition and quantitatively large magnetocaloric effect, both the compounds reveal significant relative cooling power and refrigerant capacity. However, in the low temperature region, different nature in magnetocaloric effect was addressed by considering the field induced modification of short-range ordering.

1. Introduction

To elucidate the effect of external perturbations like the magnetic field, temperature, pressure, etc. on the modification of the magnetic ground state configuration, magnetocaloric effect (MCE) can be used as one of the most powerful tool [1–4]. MCE is defined by the change of both isothermal magnetic entropy or adiabatic temperature of any magnetic materials when it is subjected in a static magnetic field [5]. For a feeble change in magnetic configuration, sometimes the signature was hindered in the bulk magnetization measurements. In contrast to that, the significantly amplified response of such weak transition is appear in the magnetocaloric effect [6–8]. After the discovery of MCE in the year 1881, it was extensively studied during a few decades in the materials having large magnetic moments [9]. Generally, the materials associated with the large magnetic moment reveals a significantly large magnetocaloric effect which is a beneficial aspect from technological perspectives [10]. Regarding this context, the magnetocaloric effect of Gadolinium (Gd) and Gd-based intermetallic compounds are very well reported [11–16]. However, to use as a magnetic refrigerant, chemical stability, lower production cost, nontoxic, and insulating nature are also very crucial properties. Considering those context, doped perovskite manganite (oxide sample) gets an immense attraction over the intermetallic compounds from fundamental as well as technological perspectives [17–22]. The strong coupling between spin, charge and lattice

initiates many intriguing physical properties in doped perovskite manganite compounds. Unlike the undoped manganite, doped compounds exhibit metal–insulator transition, pronounced ferromagnetism, charge-orbital ordering, colossal magnetoresistance (CMR), large MCE and many more. Charge ordering is the real space ordering of Mn^{3+} and Mn^{4+} ions in a crystal. Below charge ordering transition temperature (T_{CO}), an antiferromagnetic-insulating state generally appears in manganite compounds [23–26].

There are several studies regarding the magnetocaloric effect in the vicinity of paramagnetic to long range ferromagnetic or antiferromagnetic transition regions. In both the cases, random magnetic moments (in the paramagnetic state) converted to highly ordered state resulting in a significantly large change in magnetic entropy at the vicinity of the transition temperature region [27–32]. The span of the transition (in temperature scale) depends on the existence of the local disorder and distribution of the ordering temperature of the local domains [33–37]. In contrast to the ferromagnetic or antiferromagnetic materials having long range magnetic ordering, the temperature dependence of MCE might be distinct in case of the glassy magnetic systems. Depending upon the glassiness of the materials, several types of spin relaxation scenario has been observed, corroborates various form of MCE responses [38–42]. In the context of MCE, another important phenomenon brings a lot of attention in the study of MCE in manganite compounds is the magnetic field induced meta-magnetic transition. The

* Corresponding author.

E-mail address: dipak.mazumdar@saha.ac.in (D. Mazumdar).

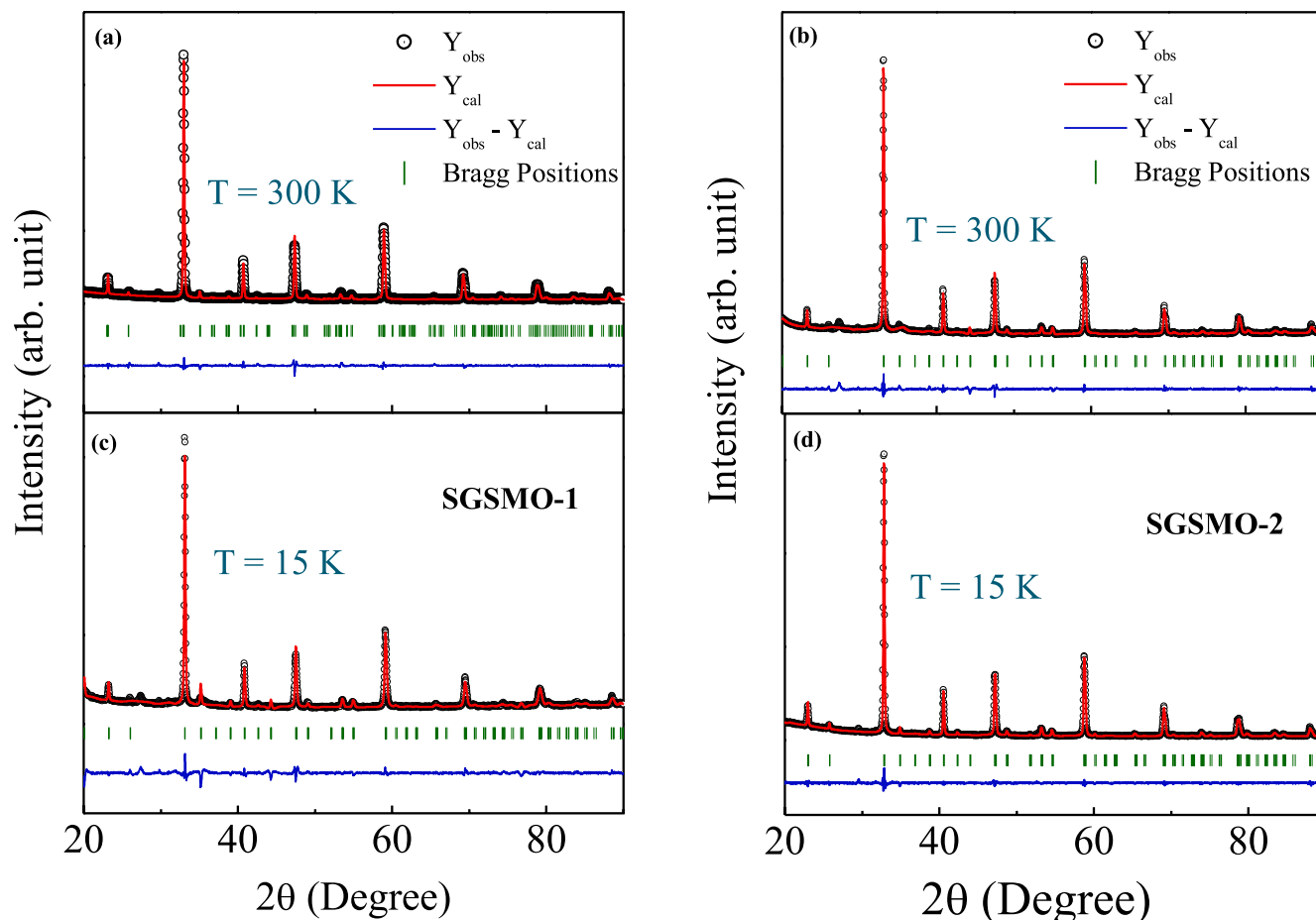


Fig. 1. (a) and (c) Profile fitted X-ray diffraction spectrum of SGSMO-1 recorded at $T = 300$ K and $T = 15$ K respectively, (b) and (d) Profile fitted X-ray diffraction spectrum of SGSMO-2 recorded at $T = 300$ K and $T = 15$ K respectively. In all the figures, the black circle represents the experimental data points and the red line is the as simulated curve generated from profile fitting. The deviation of the experimental data points from the simulated results is represented by the blue line and the olive straight line corresponds to the respected Bragg positions. (For interpretation of the references to colour in this figure legend, the reader is referred to the web version of this article.)

Table 1

The refined lattice parameters of the powdered SGSMO-1 and SGSMO-2 compounds recorded at room temperature ($T = 300$ K) and low temperature ($T = 15$ K) having space group $Pbmn$.

Compounds	T (K)	a (Å)	b (Å)	c(Å)	V (Å ³)
SGSMO-1	15	5.413	5.409	7.646	223.897
	300	5.497	5.423	7.671	228.779
SGSMO-2	15	5.411	5.407	7.650	223.855
	300	5.430	5.429	7.659	225.808

meta-magnetic transition markedly influences the magnetocaloric properties of several magnetocaloric materials [7,19,43–45].

In this present work, we aim to study the influence of short range nature of the charge-orbital ordering on the magnetic and magnetocaloric properties of manganite compounds. To serve our purpose, we have selected $(\text{Sm}_{1-y}\text{Gd}_y)_{0.55}\text{Sr}_{0.45}\text{MnO}_3$ ($y = 0.5$ and 0.7) compounds. According to the earlier reports, the short range nature of charge-orbital ordering is gradually suppressed with a decrease of temperature and vanished below the metal-insulator transition for $(\text{Sm}_{0.5}\text{Gd}_{0.5})_{0.55}\text{Sr}_{0.45}\text{MnO}_3$ compound [46]. However, it is present (in the low temperature region) in the case of $(\text{Sm}_{0.3}\text{Gd}_{0.7})_{0.55}\text{Sr}_{0.45}\text{MnO}_3$ compound [47]. At the low temperature region, ferromagnetic and spin glass nature was found for $y = 0.5$ and $y = 0.7$ compound respectively. Moreover, both the compounds show the field-induced pronounced ferromagnetism from their respective ground states [47].

Our study reveals that the magnetic and magnetocaloric properties are influenced by the modification of the short range ordering present in the compounds. Additionally, significantly large magnetocaloric effect along with large magnetic cooling capacity (both relative cooling power and refrigerant capacity) has been observed which may be beneficial from the application aspects.

2. Experimental details

Conventional solid-state reaction mechanism has been employed to prepare polycrystalline $(\text{Sm}_{1-y}\text{Gd}_y)_{0.55}\text{Sr}_{0.45}\text{MnO}_3$ ($y = 0.5$ and 0.7) (SGSMO) compounds. To prepare the compounds, we used high purity based Sm_2O_3 (99.99%), Gd_2O_3 (99.99%), SrCO_3 (99.995%) and MnO_2 (99.9%) powders as precursors. Both the rare-earth oxides were pre-heated at 800°C for 12 h. to get rid of any water vapor or CO_2 present in it. The stoichiometric mixture of all the compounds was calcined in the temperature range of $900^\circ\text{C} - 1200^\circ\text{C}$ for 60 h. with several intermediate grinding for chemical homogenization. Finally, the sintering powder was pelletized using hydrostatic pressure and again sintered at 1350°C for another 30 h and the furnace was cooled down slowly to room temperature.

Both low temperature (down to 15 K) and room temperature X-ray diffraction (XRD) pattern were recorded on the powder samples by using $\text{Cu-K}\alpha$ radiation in the Rigaku-TTRAX-III diffractometer to ensure the crystallographic phases as well as the homogenization nature of the compound. The phase purity and crystal structure were checked by

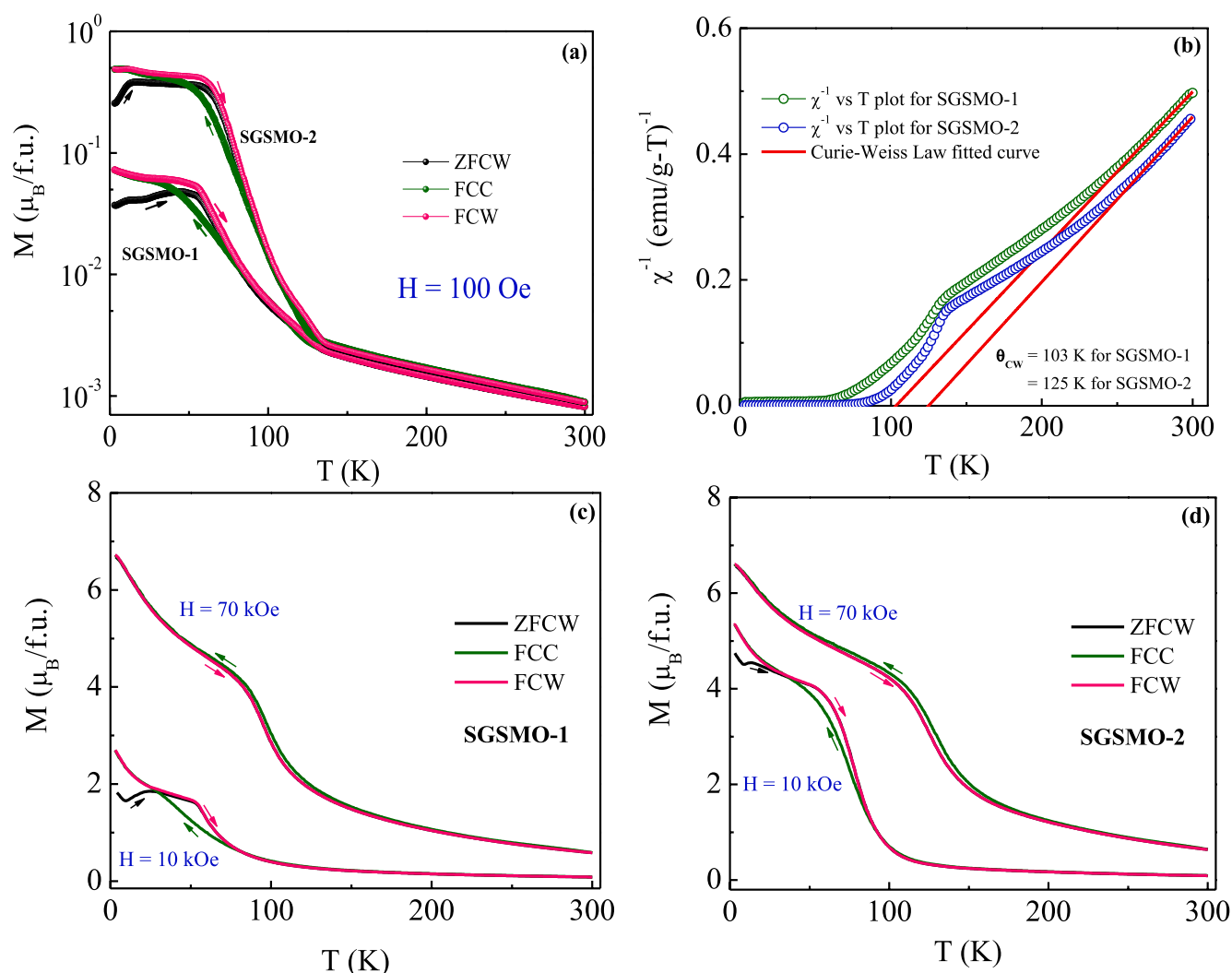


Fig. 2. (a) Temperature dependence of magnetization (M - T) recorded for the two samples SGSMO-1 and SGSMO-2 under the application of an external magnetic field of $H = 100$ Oe in three different protocols viz. ZFCW, FCC, and FCW, (b) Reciprocal of susceptibility as a function of temperature along with the Curie-Weiss law fitted curve at the high temperature region (represented by red lines) in presence of 100 Oe magnetic field for both the compounds SGSMO-1 and SGSMO-2; (c) and (d) shows the variation of magnetization with temperature under the application of 10 kOe and 70 kOe magnetic field for SGSMO-1 and SGSMO-2 compounds respectively. Arrows are used for the guidance of the observer. (For interpretation of the references to colour in this figure legend, the reader is referred to the web version of this article.)

Rietveld analysis (only profile fitting) of the as-recorded XRD spectrum using the FULLPROF software package. To measure the magnetic properties of the compounds, both vibrating sample mounting based Super Conducting Quantum Interference Device (SQUID-VSM) and physical property measurement system (PPMS) from Quantum Design have been utilized. For the sake of clarity in the main text, $(\text{Sm}_{1-y}\text{Gd}_y)_{0.55}\text{Sr}_{0.45}\text{MnO}_3$, $y = 0.7$ is denoted as SGSMO-1 and $(\text{Sm}_{1-y}\text{Gd}_y)_{0.55}\text{Sr}_{0.45}\text{MnO}_3$, $y = 0.5$ is by SGSMO-2.

3. Results and discussions

Both room temperature and low temperature ($T = 15$ K) powder X-ray diffraction (XRD) spectrums of SGSMO-1 and SGSMO-2 compounds (Fig. 1) reveal that the Bragg peaks in the diffraction pattern can be well indexed with orthorhombic crystal structure having $Pbnm$ (No. 62) space group symmetry. Additionally, the compounds are formed in single-phase without any additional impurity phase. The low-temperature XRD spectrums indicate that the absence of any structural change in the compounds with decreasing the temperature down to 15 K. The refined lattice parameters for both the compounds are

summarized in Table 1. The unit cell volume (V) decreases with decreasing temperature down to 15 K due to the thermal shrink of the unit cell with reduction of temperature.

To elucidate the temperature and magnetic field dependent response of the magnetic state, we have measured magnetization as a function of temperature for both the compounds in three different protocols which are as follows:

- **Zero Field Cooled Warming (ZFCW):** The sample was first cooled down from 300 K to 5 K in the absence of an external magnetic field. After reaching the low temperature, the desired external magnetic field was applied and magnetization data were recorded during the warming cycle.
- **Field Cooled Cooling (FCC):** In this measurement technique, the desired amount of magnetic field was applied at the room temperature (paramagnetic state of the sample) and temperature dependence of magnetization data were recorded during cooling from 300 K to 5 K with the magnetic field.
- **Field Cooled Warming (FCW):** Desired external magnetic field was applied at room temperature and the sample was allowed to

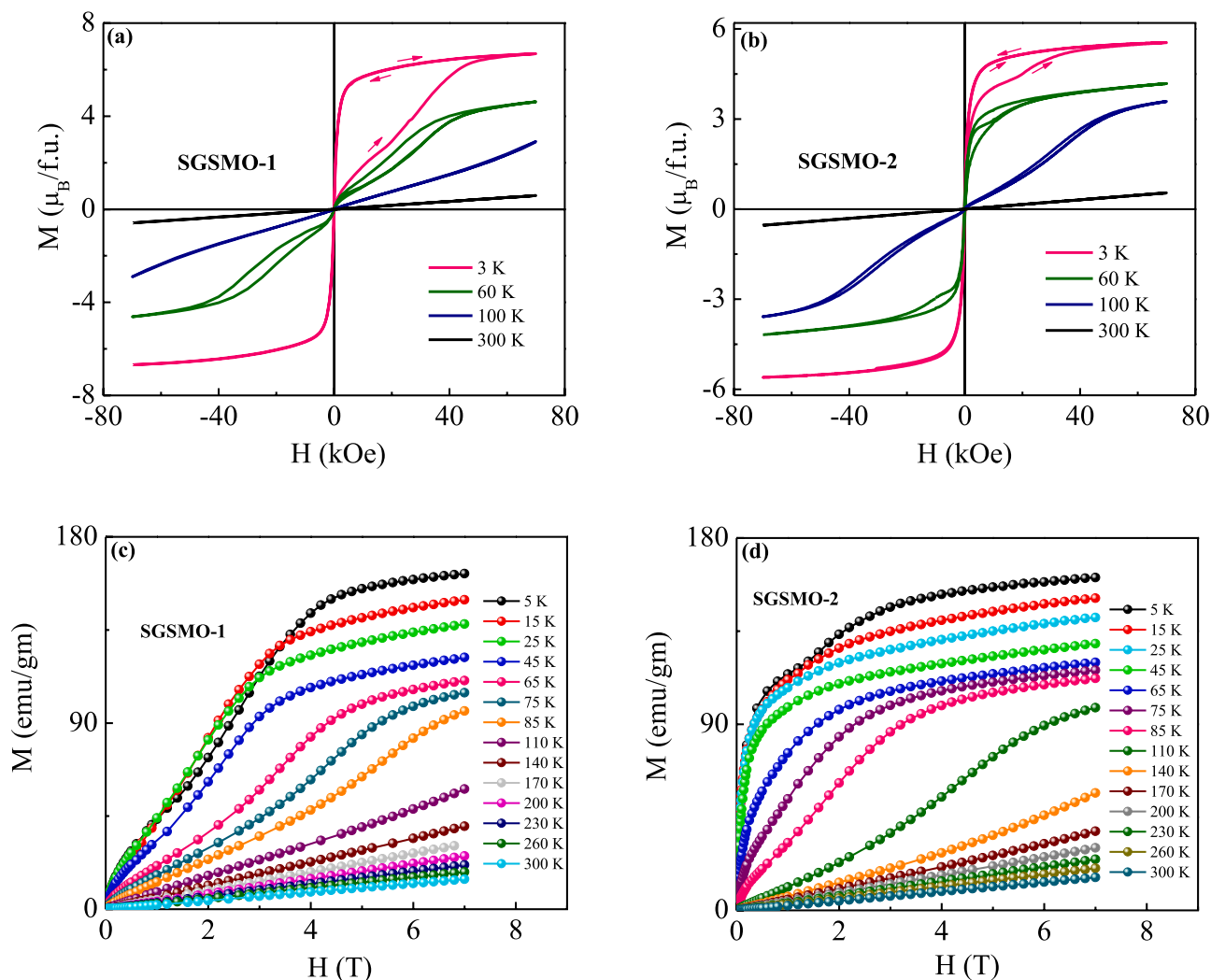


Fig. 3. Variation of magnetization with the applied external magnetic field recorded at $T = 3\text{ K}, 60\text{ K}, 100\text{ K},$ and 300 K for (a) SGSMO-1 and (b) SGSMO-2 compounds. Isothermal magnetization as a function of the applied magnetic field (M - H) recorded at $T = 5 \rightarrow 300\text{ K}$ with an interval of 10 K over the field change of $0 \rightarrow 70\text{ kOe}$ for (c) SGSMO-1 and (d) SGSMO-2 compounds. (We have plotted magnetic isotherms for some selected temperatures for sake of clarity).

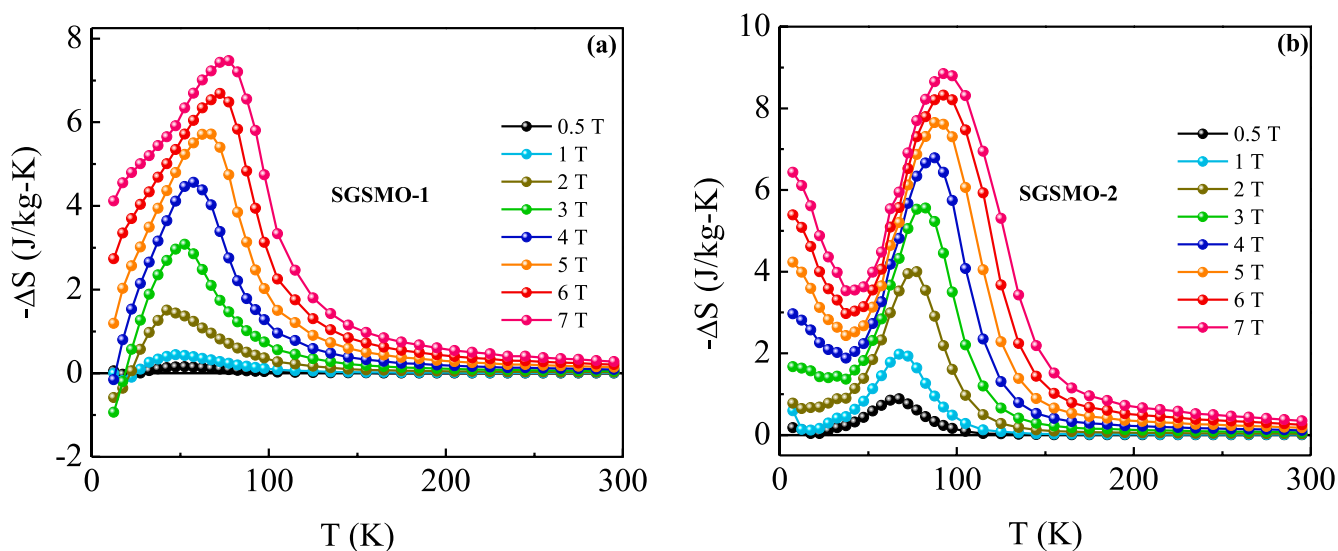


Fig. 4. Variation of magnetic entropy change ($-\Delta S$) with respect to temperature for different magnetic fields for (a) SGSMO-1 and (b) SGSMO-2 compound.

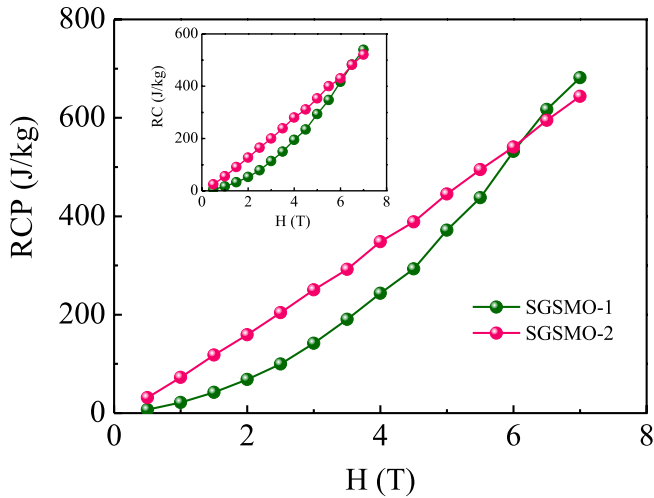


Fig. 5. Variation of relative cooling power (RCP) with applied external magnetic fields for SGSMO-1 and SGSMO-2 compounds. The inset shows the magnetic field dependence of refrigerant capacity (RC) for both the compounds.

Table 2

Comparison of magnetocaloric parameters (ΔS_{max} and RCP) of the present studied systems along with some other perovskite type oxide materials and Gd-based intermetallic compounds.

Compounds	T_C (K)	ΔS_{max} (J/kg.K)	H (T)	RCP J/kg	References
SGSMO-1	58.8	7.45	7	682	Present work
SGSMO-2	70.5	8.84	7	644	Present work
$La_{0.7}Sr_{0.3}Mn_{0.98}Ni_{0.02}O_3$	350	7.65	7	459	[22,51]
$La_{0.66}(Ca/Pb)_{0.33}MnO_3$	290	7.5	7	375	[22,52]
$La_{0.845}Sr_{0.155}MnO_3$	234	6.6	7	396	[22,53]
$La_{0.815}Sr_{0.185}MnO_3$	280	7.1	7	533	[22,54]
$La_{0.7}Ca_{0.25}Sr_{0.05}MnO_3$	275	10.5	5	462	[22,55]
$La_{1.4}Ca_{1.6}Mn_2O_7$	270	16.8	5	420	[22,56]
Gd	294	10.2	5	410	[57]
$Gd_5Si_2Ge_2$	276	18.4	5	535	[57]
$GdZn_2$	85	11.5	7	690	[58]
$GdMnO_3$	40	15	7	211	[59]
GdAlO ₃	(T_N) 3.9	3.4	7	203	[59]
	(T_N)				

cool down in the presence of that applied magnetic field. After reaching the low temperature, temperature-dependent magnetization data were recorded during the warming cycle.

The above-mentioned history-dependent magnetization measurement technique played a very important role to understand the magnetic ground state especially for the compound where phase competing nature and short-range ordering are present [2]. Temperature dependent magnetization in the presence of $H = 100$ Oe external magnetic field is shown in Fig. 2(a). Magnetization response of the two compounds reveals that the ferromagnetic fractions are oriented below $T = 150$ K temperature. However, the growth of the magnetization below 150 K is more pronounced in the SGSMO-2 sample compare to SGSMO-1. It should also be noted that a quantitatively lower magnetization value was observed in a higher Gd-content sample. A thermal hysteresis has been observed in between FC curves corresponding to the first-order magnetic phase transition (FOPT) in the system [48]. In case of both the systems, an anomaly has been observed in ZFCW curve near $T \sim 13$ K. This anomaly may arise due to the antiferromagnetic arrangement of Gd sublattices [49]. For visualization of the presence of ferromagnetic interaction, we have plotted temperature dependent inverse susceptibility as shown in Fig. 2(b) and fitted the high temperature paramagnetic region with the Curie–Weiss (CW) law of the form χ

$= C/(T - \theta_{CW})$, where $C = \mu_{eff}^2/3k$ is the Curie constant and θ_{CW} represents the Curie–Weiss temperature. The extrapolated linear part from the paramagnetic region indicates that the paramagnetic Curie temperature (θ_{CW}) is higher in SGSMO-2 compound which again indicates the stronger ferromagnetic interaction present in this compound. The higher values of experimentally estimated effective magnetic moment, $(\mu_{eff})_{exp}$ ($\sim 8.12 \mu_B/f. u.$ for SGSMO-1 and $\sim 8 \mu_B/f. u.$ for SGSMO-2) compared to the theoretically calculated effective magnetic moment $(\mu_{eff})_{theo}$ ($\sim 6.65 \mu_B/f. u.$ for SGSMO-1 and $\sim 6.12 \mu_B/f. u.$ for SGSMO-2) indicates the presence of short-range ferromagnetic type clusters in the paramagnetic background of the compounds [19]. As reported earlier, spin glass nature is dominant in the SGSMO-1 compound at low temperature (in the presence of lower value of the magnetic field) [47]. In our present study, comparatively slightly larger bifurcation between the ZFCW and FCW at a low magnetic field ($H = 100$ Oe) may be associated with the glassy nature of the compound. Magnetization as a function of temperature in the presence of $H = 10$ and 70 kOe was shown in Fig. 2(c) and Fig. 2(d) for SGSMO-1 and SGSMO-2 respectively. At $H = 10$ kOe, the predominant ferromagnetism is clearly visualized in case of the SGSMO-2 compound and it is small for SGSMO-1 compound. That is the contribution of Gd sublattices enhances with the magnetic field resulting in the higher value of magnetization. However, in the presence of $H = 70$ kOe external magnetic field, magnetization rapidly increases in both the compounds and non saturating nature were observed. Additionally, the bifurcation between the three different protocols is also disappeared which may be associated with the result of field induced meta-magnetic transition.

To get a better view of the modification of the magnetic ground state for both the compounds under the application of an external magnetic field, isothermal magnetization measurements have been performed and as presented in Fig. 3. The five quadrants (0 kOe \rightarrow 70 kOe \rightarrow -70 kOe \rightarrow 70 kOe) hysteresis loops at different temperatures are plotted in Fig. 3 (a) and (b) for SGSMO-1 and SGSMO-2 compounds respectively. One can notice the dramatic change of the M-H curves for different temperatures. Both the systems undergo a field-induced metamagnetic like transition. The required magnetic field for such metamagnetic like transition is lower in case of the SGSMO-2 compound compared to the SGSMO-1 compound having a glassy magnetic state. A pronounced magnetic field hysteresis between increasing and decreasing field has been observed in both the compounds at $T = 60$ K and 100 K. Whereas, negligible hysteresis has been observed at $T = 3$ K. Presence of S-shaped behavior of the M-H curves and field hysteresis indicate the signature of first-order metamagnetic phase transition in both the compounds [48]. However, after the field induced metamagnetic transition, the compounds exhibit soft ferromagnetic like nature during subsequent field cycling. At 300 K, thermal energy helps to lose the blockage of magnetic spins, resulting in the randomness of magnetic spins and the system converted into paramagnetic one which is reflected in the M-H curves [19].

In order to study the magnetocaloric effect, one quadrant magnetic isotherms were recorded for different temperatures as depicted in Fig. 3(c) and (d) for SGSMO-1 and SGSMO-2 compounds respectively. The one quadrant field dependent magnetization data again point out about the higher field requirement for meta-magnetic transition in case of SGSMO-1 compound compared to the SGSMO-2 compound.

In case of a magnetic material, the net change of magnetic entropy value (ΔS) due to the sweeping of magnetic field from 0 to H can be estimated by utilizing the classical Maxwell's thermodynamic relation which is expressed as [50],

$$\Delta S = \int_0^H \left(\frac{\partial M}{\partial T} \right) dH \quad (1)$$

The temperature dependence of magnetic entropy change ($-\Delta S$) for the change of various field values both for SGSMO-1 and SGSMO-2 compounds have been presented in Fig. 4(a) and (b) respectively.

Although the value of $-\Delta S$ is positive in the whole temperature range for both of the compounds, some anomalies can be identified in $-\Delta S$ vs. T plots depending on the ground state of the compounds. Due to the presence of spin-glassy nature in the ground state of the SGSMO-1 compound at low-temperature regions, asymmetric nature of $-\Delta S$ vs T plots has been observed. The short-range ordering of cations leads to generate more likely a table-like nature in the $-\Delta S$ vs T curves within a very small temperature scale and this asymmetric wide broadening of $-\Delta S$ is sufficient to achieve higher values of the refrigerant capacity of the SGSMO-1 compound. Interestingly, distinct behavior of $-\Delta S$ vs. T plots has been noticed in the case of the SGSMO-2 compound. An anomaly has been observed in the $-\Delta S$ vs. T curves below $T < 50$ K although the compound exhibited long-range ordered ferromagnetic ground state at low temperature. This strong anomaly shows the sharp increment of $-\Delta S$ values with increasing magnetic field values. The transition temperature (T_C) shifted towards high temperature for both of the compounds indicating the presence of ferromagnetic interaction either in short-range scale (SGSMO-1) or in long-range order (SGSMO-2). Relatively higher values of $-\Delta S$ can be observed in case of SGSMO-2 ($-\Delta S = 8.84$ J/kg-K for $\Delta H = 7$ T) compared to SGSMO-1 ($-\Delta S = 7.45$ J/kg-K for $\Delta H = 7$ T) where the concentration of Gd is high. Fig. 5.

In order to evaluate the magnetic cooling capacity of any magnetic materials, there are two parameters namely, relative cooling power (RCP) and refrigerant capacity (RC) are widely used in the cooling technology. Basically, the cooling capacity of a material is the net amount of heat transfer between a cold sink and a hot source in an ideal refrigeration cycle. The value of both RCP and RC strongly depends on the maximum value of $-\Delta S$ and the broadening of $-\Delta S$ vs. T curves. RCP can be calculated numerically by multiplying the maximum value of $-\Delta S$ ($-\Delta S_{max}$) and the δT at full-width at half maxima (FWHM) of the $-\Delta S_{max}$ value at temperature scale. Alternately, RC can be estimated within a temperature range δT (where $\delta T = T_2 - T_1$) using the following relation

$$RC = \int_{T_1}^{T_2} |\Delta S| dT \quad (2)$$

The variation of the RCP concerning magnetic field is shown in the main panel of Fig. 5 and the inset shows the magnetic field dependence of RC. We have achieved high values of RCP (and RC) for both of the compounds compared to other similar types of materials. For comparison, we have summarized the magnetocaloric parameters of the studied systems along with some other similar types of compounds as presented in Table 2. Interestingly, RCP (and RC) values vary linearly and almost quadratically with applied fields in the case of SGSMO-2 and SGSMO-1 compounds respectively. An asymmetric nature of $-\Delta S$ vs. T in SGSMO-1 curves may lead to the deviation of RCP (and RC) from its linear dependence of field values. The ferromagnetic ground state of SGSMO-2 helps to get uniform broadening of $-\Delta S$ vs. T curves and as a result we get a linear dependence of δT values along with fields. Therefore, the short-range interaction present in the spin-glassy SGSMO-1 compound mediated the broadening and as a result we get higher value of RCP (682 J/kg for $\Delta H = 7$ T) although the maximum value of $-\Delta S$ is small compared to SGSMO-2. From the above discussion, we can conclude that the Gd-doping concentration highly influence the magnetic ground state of both the SGSMO compounds.

4. Conclusions

To summarize, we have performed the magnetic and magnetocaloric effect study for the polycrystalline $(\text{Sm}_{1-y}\text{Gd}_y)_{0.55}\text{Sr}_{0.45}\text{MnO}_3$ ($y = 0.5$ and 0.7) (SGSMO) compounds prepared by well-known solid-state reaction method. No structural transformation has been noticed for both the compounds, confirmed from the successive profile fitted X-ray diffraction data down to 15 K. Experimental outcomes indicate that irrespective of the meta-magnetic transition, the magnetocaloric effect

is influenced drastically depending upon their ground state. Significantly large magnetocaloric effect was observed even in lower Gd-content sample. Additionally, large values of both relative cooling power and refrigerant capacity make the compounds suitable candidates from the view of technological importance in the refrigeration industry.

Declaration of Competing Interest

The authors declare that they have no known competing financial interests or personal relationships that could have appeared to influence the work reported in this paper.

Acknowledgements

The work was supported by the Department of Atomic Energy (DAE), Govt. of India.

References

- [1] H. Zhu, C. Xiao, H. Cheng, F. Grote, X. Zhang, T. Yao, Z. Li, C. Wang, S. Wei, Y. Lei, Yi Xie, Nat. Commun. 5, (2014) 3960.
- [2] T. Paramanik, T. Samanta, R. Ranganathan, I. Das, RSC Adv. 5 (2015) 47860.
- [3] F. Cugini, G. Porcari, S. Fabbri, F. Albertini, M. Solzi, Philos. Trans. R. Soc. A 374 (2016) 20150306.
- [4] D.M. Polishchuk, Yu.O. Tykhonenko-Polishchuk, E. Holmgren, A.F. Kravets, A.I. Tovstolytkin, V. Korenivski, Phys. Rev. Mater. 2 (2018) 114402.
- [5] A.M. Tishin, K.H.J. Buschow (Ed.), Handbook of Magnetic Materials, vol. 12, North-Holland, Amsterdam, 1999, p. 395.
- [6] T. Paramanik, K. Das, T. Samanta, I. Das, J. Magn. Magn. Mater. 381 (2015) 168.
- [7] D. Mazumdar, K. Das, S. Roy, I. Das, J. Magn. Magn. Mater. 497 (2020) 166066.
- [8] K. Das, N. Banu, I. Das, B.N. Dev, J. Magn. Magn. Mater. 487 (2019) 165309.
- [9] A. Smith, Euro. Phys. J. H 38 (2013) 507.
- [10] M.E. Wood, W.H. Potter, Cryogenics 25 (1985) 667.
- [11] V.K. Pecharskya, K.A. Gschneidner Jr., Appl. Phys. Lett. 70 (1997) 3299.
- [12] V.K. Pecharsky, K.A. Gschneidner Jr., Phys. Rev. Lett. 78 (1997) 23.
- [13] X.J. Niua, K.A. Gschneidner Jr., A.O. Pecharskya, V.K. Pecharskya, J. Magn. Magn. Mater. 234 (2001) 193.
- [14] W. Dai, B.G. Shen, D.X. Li, Z.X. Gao, J. Alloys and Comp. 311 (2000) 22.
- [15] K.A. Gschneidner Jr., V.K. Pecharsky, Mater. Sci. Eng.: A 287 (2000) 301.
- [16] K.T. Matsumoto, K. Hiraoka, J. Magn. Magn. Mater. 423 (2017) 318.
- [17] K.A. Gschneidner Jr., V.K. Pecharsky, A.O. Tsokol, Rep. Prog. Phys. 68 (2005) 1479.
- [18] K. Das, I. Das, J. Appl. Phys. 119 (2016) 093903.
- [19] D. Mazumdar, K. Das, I. Das, J. Magn. Magn. Mater. 502 (2020) 166507.
- [20] A. Asamitsu, Y. Tomioka, H. Kuwahara, Y. Tokura, Nature 388 (1997) 50.
- [21] J.D. Hoffman, M.S. Wu, B.J. Kirby, A. Bhattacharya, Phys. Rev. Appl. 9 (2018) 044041.
- [22] M.H. Phan, S.C. Yu, J. Magn. Magn. Mater. 308 (2007) 325.
- [23] Y. Tokura, Y. Tomioka, J. Magn. Magn. Mater. 200 (1999) 1.
- [24] A. Arulraj, P.N. Santhosh, R. Srinivasa Gopalan, A.K. Ayan Guha, N. Kumark Raychaudhuri, C.N.R. Rao, J. Phys. Condens. Mater. 10 (1998) 8497.
- [25] Y. Tokura, Rep. Prog. Phys. 69 (2006) 797.
- [26] S. Banik, K. Das, T. Paramanik, N.P. Lalla, B. Satpati, K. Pradhan, I. Das, NPG Asia Mater. 10 (2018) 923.
- [27] K. Das, S. Banik, I. Das, Mater. Res. Bull. 73 (2016) 256.
- [28] A. Mleiki, S. Othmani, W. Cheikhrouhou-Koubaa, A. Cheikhrouhou, E.K. Hliil, J. Alloys Comp. 688 (2016) 1214.
- [29] S.K. Giri, P. Dasgupta, A. Poddar, A.K. Nigam, T.K. Nath, J. Alloys Comp. 582 (2014) 609.
- [30] K. Das, S. Banik, I. Das, Physica B: Condensed Matter 533 (2018) 46.
- [31] A. Midya, S.N. Das, P. Mandal, S. Pandya, V. Ganesan, Phys. Rev. B 84 (2011) 235127.
- [32] A. Rostamnejadi, M. Venkatesan, P. Kameli, H. Salamati, J.M.D. Coey, J. Magn. Magn. Mater. 323 (2011) 2214.
- [33] J.M. De Teresa, M. Ibarra, J. Garcia, J. Blasco, C. Ritter, P. Algarabel, C. Marquina, A. del Moral, Phys. Rev. Lett. 76 (1996) 3392.
- [34] S. Banik, I. Das, J. Alloys and Comp. 742 (2018) 248.
- [35] J. Khelifi, A. Tozri, E. Dhahri, Appl. Phys. A 116 (2014) 1041.
- [36] J.P. Zhoua, J.T. McDevitt, J.S. Zhou, H.Q. Yin, J.B. Goodenough, Y. Gim, Q.X. Jia, Appl. Phys. Lett. 75 (1999) 1146.
- [37] M. Otero-Leal, F. Rivadulla, J. Rivas, Phys. Rev. B 76 (2007) 174413.
- [38] K.F. Wang, Y. Wang, L.F. Wang, S. Dong, D. Li, Z.D. Zhang, H. Yu, Q.C. Li, J.M. Liu, Phys. Rev. B 73 (2006) 134411.
- [39] S. Pakhira, C. Mazumdar, R. Ranganathan, S. Giri, Phys. Chem. Chem. Phys. 20 (2018) 7082.
- [40] M. Orendac, J. Hanko, E. Cizmar, A. Orendacova, M. Shirai, S.T. Bramwell, Phys. Rev. B 75 (2007) 104425.
- [41] F. Yuan, J. Du, B. Shen, Appl. Phys. Lett. 101 (2012) 032405.
- [42] J. Du, Q. Zheng, E. Bruck, K.H.J. Buschow, W.B. Cui, W.J. Feng, Z.D. Zhang, J.

- Magn. Magn. Mater. 321 (2009) 413.
- [43] T. Samanta, I. Das, S. Banerjee, Appl. Phys. Lett. 91 (2007) 152506.
- [44] S. Pakhira, C. Mazumdar, R. Ranganathan, S. Giri, M. Avdeev, Phys. Rev. B 94 (2016) 104414.
- [45] T. Samanta, I. Das, S. Banerjee, Appl. Phys. Lett. 91 (2007) 082511.
- [46] F.N. Bukhanko, Physics Research International (2012).
- [47] Y. Tomioka, Y. Okimoto, J.H. Jung, R. Kumai, Y. Tokura, Phys. Rev. B 68 (2003) 094417.
- [48] P. Sarkar, S. Arumugam, P. Mandal, A. Murugeswari, R. Thiyagarajan, S. Esaki Muthu, D. Mohan Radheep, C. Ganguli, K. Matsubayshi, Y. Uwatoko, Phys. Rev. Lett. 103 (2009) 057205.
- [49] M. Das, S. Roy, N. Khan, P. Mandal, Phys. Rev. B 98 (2018) 104420.
- [50] T. Hashimoto, T. Numasawa, M. Shino, T. Okada, Cryogenics 21 (1981) 647.
- [51] M.H. Phan, N.D. Tho, N. Chau, S.C. Yu, M. Kurisu, J. Appl. Phys. 97 (2005) 3215.
- [52] Y. Sun, M.B. Salamon, S.H. Chun, J. Appl. Phys. 92 (2002) 3235.
- [53] A. Szewczyk, M. Gutowska, K. Piotrowski, B. Dabrowski, J. Appl. Phys. 94 (2003) 1873.
- [54] A. Szewczyk, M. Gutowska, B. Dabrowski, T. Plackowski, N.P. Danilova, Y.P. Gaidukov, Phys. Rev. B 71 (2005) 224432.
- [55] M.H. Phan, S.C. Yu, N.H. Hur, Appl. Phys. Lett. 86 (2005) 072504.
- [56] H. Zhu, H. Song, Y.H. Zhang, Appl. Phys. Lett. 81 (2002) 3416.
- [57] V.K. Pecharsky, K.A. Gschneidner, A.O. Tsokol, Rep. Prog. Phys. 68 (2005) 1479.
- [58] K.T. Matsumoto, K. Hiraoka, J. Magn. Magn. Mater. 423 (2017) 318.
- [59] S. Mahana, U. Manju, D. Topwal, J. Phys. D: Appl. Phys. 50 (2017) 035002.